IOP Conf. Series: Materials Science and Engineering **382** (2018) 022027 doi:10.1088/1757-899X/382/2/022027

Characterization and the improved Arrhenius model of 0Cr11Ni$_2$MoVNb steel during hot deformation process

Jia FU[1, 2], Fuguo LI[2], Yongtang LI[3]

[1]School of Material science and engineering, Xi'an Shiyou University, Xi'an, 710065, China;

[2]School of Materials Science and Engineering, Northwestern Polytechnical University, Xi'an 710072, China;

[3]Material science and engineering, Taiyuan university of science and technology, taiyuan, 030024, China;

Email: fujia@xsyu.edu.cn

Abstract: True stress versus true strain curves of 0Cr11Ni$_2$MoVNb alloy steel were obtained from isothermal compression tests on Gleeble-1500 tester over a wide temperature range from 1223K to 1433K and a strain rate range from 0.01s^{-1} to 10s^{-1}. Considering the compensation of strain, the improved Arrhenius model based on Zener–Holloman parameter was evaluated by regression analysis and modified by optimizing parameters of strain hardening exponent as well as the deformation activation energy with a method of five-order polynomial fitting. Then constitutive equation of the flow stress was verified by comparing both the correlation coefficient R and the average absolute relative error (AARE). The main result shows that: (1) the deformation activation energy is insensitive to strain rate under a lower temperature range from 1223K to 1373K; (2) maximum values of the deformation activation energy under various strain degree are concentrated with the temperature over 1373K and the strain rate nearby 0.1s^{-1}. (3) the improved Arrhenius model has a low value level of its parameters R(<0.977%) and AARE (<5.031%), which has a good agreement with the experimental values to predict the flow stress at different temperatures and strain rates.

1. Introduction

0Cr11Ni$_2$MoVNb is a new kind of martensitic stainless steel, which is a kind of hot rolled steel achieved by heat treatment (quenching and tempering) to adjust the performance of stainless steel, with high strength and corrosion resistance. The martensitic stainless steel can be used to make working under high temperature parts, such as steam turbine blades, gear shaft and pull rod and parts such as valve working in corrosion medium, bolts, large gas turbine engine turbine disc, etc. [1, 2]. Material physical parameters can be calculated through various simulation methods to provide support for performance calculation [3-7]. In general, constitutive models of metallic materials are usually used to predict the flow stress, to help to establish the recrystallization model and grain size model for the study of dynamic behavior. It is the necessary condition to calculate the plastic deformation process, create a mathematical model for thermal deformation behavior of materials under high temperature. The influence of the thermal deformation condition on the flow stress curve can be obtained by analyzing the test data. The constitutive model provides the theoretical basis for the efficient production of high quality, thus can be used to optimize hot working performance and control

the microstructure of material.

At present, the research on constitutive equation of metal material commonly use the hyperbolic sine function to select the peak stress strain, with Z parameters represent temperature, strain rate and the relationship among stress, ignoring the effect of strain on the constitutive equation of material constant. Commonly, the flow stress gradually increases to a peak (initial strain hardening) and then decreases slowly to a steady state. Such flow stress behavior is a typical characteristic of hot working that is accompanied by dynamic recrystallization softening.vGuoliang Ji et al. have used Arrhenius-type constitutive model and artificial neural network model to evaluate and predict the high-temperature deformation behavior of Aermet100 steel [8-10]. This paper adopt a new method [11-13], through adding the strain compensation, the constitutive relationship among temperature, strain, strain rate and stress is established to predict deformation behavior of 0Cr11Ni$_2$MoVNb steel at high temperature. In this paper, the strain rate and temperature were controlled in the thermal compression test, and the stress-strain data of the material were obtained. The improved Arrhenius model of 0Cr11Ni2MoVNb steel during hot deformation process was established.

2. Experimental material and procedure

The chemical compositions of 0Cr11Ni$_2$MoVNb stainless steel were (wt.%): C: 0.070, Si: 0.180, Mn: 0.380, Cr: 11.39, Ni: 1.570, Mo: 0.390, V: 0.150, Nb: 0.080, P: 0.015, S: 0.004, Fe: (balance). Cylindrical specimens with a diameter of 8 *mm* and a height of 12 *mm* were machined and with grooves of 0.2mm depth on both sides filled with graphite powder as lubricant to reduce friction and assure the stability and uniformity during compression testing. A computer-controlled, servo-hydraulic Gleeble 1500 machine was used for compression testing with height reduction 80% at the temperatures of 1223K, 1273K, 1323K, 1373K and 1433K, and the strain rates of 0.01 s^{-1}, 0.1 s^{-1}, 1 s^{-1} and 10 s^{-1}. These 20 specimens were heated to 1473K at first at a heating rate of 283K/s with holding time 180s and cooled to deformation temperatures selected for the corresponding compression, and then specimens were isothermally compressed at the constant strain rates and then rapidly quenched with water to room temperature. The variations of stress and strain were recorded automatically by a personal computer equipped affixed to an automatic data acquisition system during isothermal compression. The true stress–strain curves were calculated by the related formula [14] and the nominal stress–strain curves.

3. Results and discussion

3.1 Analysis of experimental stress-strain curves

The true stress-strain curves of 0Cr11Ni$_2$MoVNb obtained by hot compression test are depicted in Figure 1.

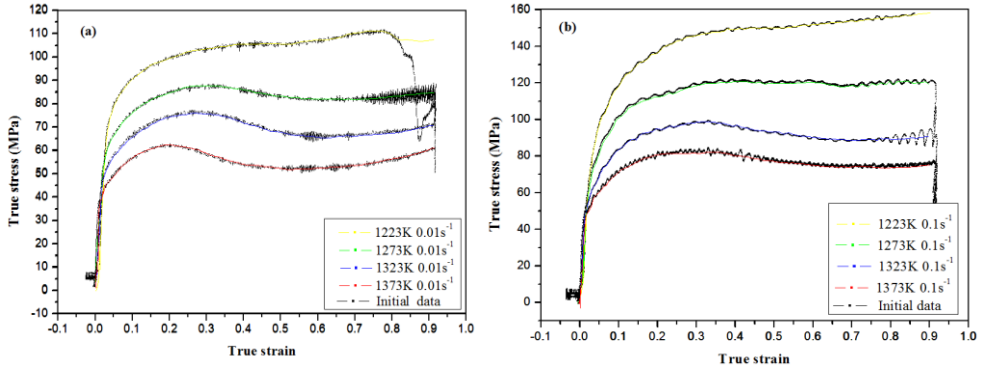

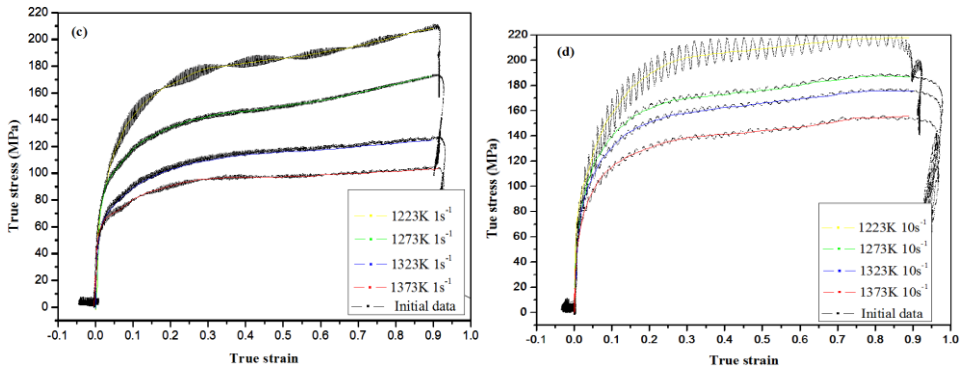

Figure 1 Flow curves of 0Cr11Ni$_2$MoVNb steel under various conditions: (a) 0.01s^{-1}; (b) 0.1s^{-1}; (c) 1s^{-1}; (d) 10s^{-1}.

As is in Figure 1, the flow stress and the shape of the flow curves are sensitively dependent on temperature and strain rate. The rheological stress curve of the 0Cr11Ni2MoVNb steel under high temperature deformation has two forms: one is the high strain rate and the low deformation temperature, and the dynamic response is presented; the other is the dynamic recrystallization with low strain rate and high deformation temperature. Test results show the typical curve of dynamic recrystallization, with the characteristics: when the strain rate lower than 0.1 s^{-1} and temperature higher than 1273K, with the increase of strain, stress peak of the stress-strain curve is reached, and then followed by softening stage. In most instances, the stress level decreases with increasing of temperature and strain rate decreasing because lower strain rate and higher temperature provide longer time for the energy accumulation and higher mobilities at boundaries which result in the nucleation and growth of dynamically recrystallized grains and dislocation annihilation [15]. Also there exist some cases that the flow stress increases monotonically from beginning to end, showing dynamic work-hardening. The degree of dynamic softening is considerably light during deformation at the cases nearly horizontal lines are obtained, which suggests that thermal softening is being balanced by work-hardening. In contrast, for a fixed temperature, the flow stress generally increases as the strain rate increases due to the increase of dislocation density and the dislocation multiplication rate. When the flow stress relative to the temperature is compared to the flow stress relative to the strain rate, there is no doubt that the temperature effect on the flow stress is more pronounced.

3.2 Establish of constitutive equations considering compensation of strain

For all stress levels, the relationship among stress, strain rate and temperature described by the Arrhenius equation under various $\alpha\sigma$ values [16] can be expressed as:

$$\dot{\varepsilon} = A[\sinh(\alpha\sigma_p)]^n \exp[-Q/(RT)] \tag{1}$$

Where, $\dot{\varepsilon}$ is the strain rate (s^{-1}); T is the absolute temperature (K); R is the universal gas constant; Q is the deformation activation energy (J/mol^{-1}); A, n', β, α and n are the material constants and exists relation of $\alpha=\beta/n'$.

Zener–Holloman parameter (Z) in an exponent-type equation is employed to describe the effects of temperature and strain rate on material deformation behavior and can be expressed by equation (3).

$$Z = \dot{\varepsilon}\exp[Q/(RT)] = A[\sinh(\alpha\sigma)]^n \tag{2}$$

For a certain strain rate given, Eqs.(1) can be rewritten as

$$Q = R \cdot n \cdot \frac{\partial \ln[\sinh(\alpha\sigma)]}{\partial(1/T)} \tag{3}$$

For a certain strain rate, taking logarithm of both sides of Eqs.(1) yields,

$$\ln\left[\sinh\left(\alpha\sigma\right)\right] = \frac{1}{n}\left(\ln\dot{\varepsilon} - \ln A\right) + Q/nRT \tag{4}$$

Taking logarithm of both sides of Eqs.(2) yields,

$$\ln Z = \ln A + n \ln\left[\sinh(\alpha\sigma)\right] \tag{5}$$

Under different strain rates, the flow stress at different temperatures can be obtained by Eqs.(1), thus the relation of ln[sinh(ασ)]-1/T is obtained. For linear regression of the lnsinh($\alpha\sigma_p$) –1/T curve, the slope is obtained and the deformation activate energy Q with the same strain degree under different strain rates is averaged to be Q_1 under the strain degree. Besides, by the average slope K of the σ_p-1/T curve, the deformation activation Q_2 is calculated using the formula Q=RβK. The value Q is averaged to be 432.078kJ·mol^{-1}. The corresponding value Z is obtained by substituting the activation energy under different temperatures and strain rates into Eqs. (2).

Under certain temperature and strain, the slope of the $\ln\left[\sinh(\alpha\sigma)\right]-\ln\dot{\varepsilon}$ function curve is *n*. For the flow stress expression σ by Z parameters, the final constitutive equation can be written as:

$$\sigma = \frac{1}{\alpha}\ln\left\{(Z/A)^{1/n} + \left[(Z/A)^{2/n}+1\right]^{1/2}\right\} \tag{6}$$

Taking the strain ε=0.3 for example, the relationship diagram between $\ln(\sigma)-\ln(\dot{\varepsilon})$ and $\sigma-\ln(\dot{\varepsilon})$ shown in Figure 2, the fitted coefficient of R-Square is all above 0.95. The average value of n_1 and β is 8.19081 and 0.075406, respectively. According to the formula α=β/n_1, the value of the coefficient α is 0.009206.

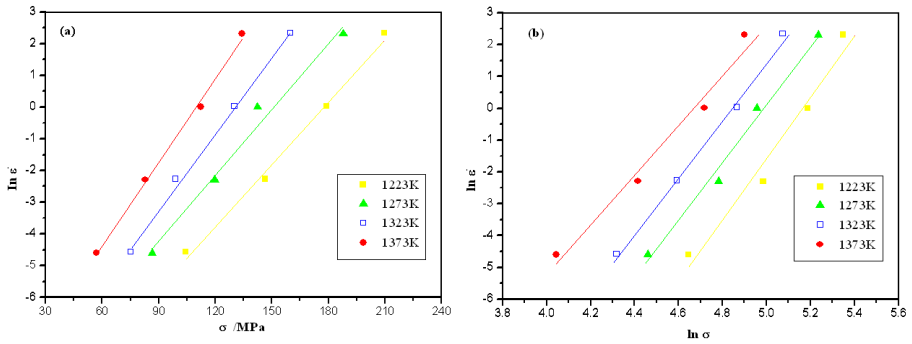

Figure 2 Parameter estimation of n_1 and β at a strain of 0.3: (a) $\ln(\sigma)-\ln(\dot{\varepsilon})$; (b) $\sigma-\ln(\dot{\varepsilon})$.

When ε=0.3, we can obtain: Q=432.078kJ·mol^{-1}. If the strain is 0.3, the lnZ-ln[sinh(ασ)] or ln[sinh(ασ)] - $\ln\dot{\varepsilon}$ can be obtained, thus the intercept lnA can be obtained and the averaged A is: A =1.8926×10^{16}.

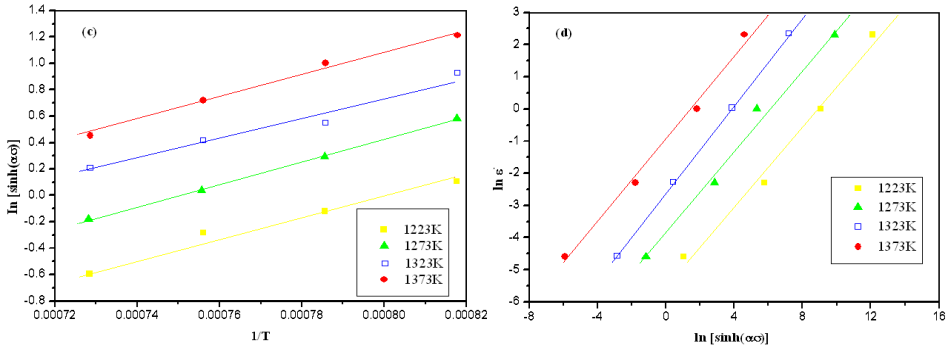

Figure 3 Parameters of *Q* and *lnA* at a strain of 0.3: (a) $\ln\left[\sinh(\alpha\sigma)\right]$ versus 1/T; (b) $\ln\left[\sinh(\alpha\sigma)\right]$ versus $\ln\dot{\varepsilon}$.

The parameters obtained from the calculation are: α=0.009206; Q=432.078kj·mol-1; n=6.7015;

A=1.8926×10^{16}. Substituting the Z-parameter expression under ε=0.3 into the Eqs.(2), thus:

$$Z = \dot{\varepsilon}\exp\left(\frac{432078}{RT}\right) \tag{7}$$

Substituting Eqs.(7) into Eqs.(6), the expression of flow stress can be described as:

$$\sigma = 108.6248\ln\left\{\left(Z/1.8926\times10^{16}\right)^{0.1647} + \left[\left(Z/1.8926\times10^{16}\right)^{0.3294}+1\right]^{1/2}\right\} \tag{8}$$

According to equation (1), the constitutive equation at a strain of 0.3 can be expressed as:

$$\dot{\varepsilon} = 1.8926\times10^{16}\left[\sinh\left(0.009206\sigma\right)\right]^{6.7015}\exp\left(\frac{-432078}{RT}\right) \tag{9}$$

Under the procedure mentioned above, material constants of α, n, Q and lnA at every interval of 0.05 in the strain range 0.05~0.85 can be repeatedly obtained. A fifth order polynomial was then adopted to fit the material constants to be the final parameters of constitutive equation.

$$\begin{aligned}
&\alpha = B_0+B_1\varepsilon+B_2\varepsilon^2+B_3\varepsilon^3+B_4\varepsilon^4+B_5\varepsilon^5\\
&n = C_0+C_1\varepsilon+C_2\varepsilon^2+C_3\varepsilon^3+C_4\varepsilon^4+C_5\varepsilon^5\\
&InA = D_0+D_1\varepsilon+D_2\varepsilon^2+D_3\varepsilon^3+D_4\varepsilon^4+D_5\varepsilon^5\\
&Q = E_0+E_1\varepsilon+E_2\varepsilon^2+E_3\varepsilon^3+E_4\varepsilon^4+E_5\varepsilon^5
\end{aligned} \tag{10}$$

Through polynomial fitting, the more accurate expression of material constant value under different strain is described. From fitting results, we can see that the material constants regularly change with the change of strain. Fitting results of parameters of *α*, *n*, *lnA* and *Q* are obtained from the polynomial is shown in Table 1.

Table 1 Coefficients of the polynomial for α, n, lnA and Q,.

α	n	lnA	Q
B_0 = 0.014	C_0 = 9.19833	D_0=40.63712	E_0=462.23694
B_1=-0.05935	C_1=-19.7946	D_1=-31.20246	E_1=-292.1756
B_2=0.24165	C_2=76.0064	D_2=128.343	E_2=1.10E+03
B_3=-0.46204	C_3=-177.875	D_3=-277.4288	E_3=-2.08E+03
B_4=0.42033	C_4=200.8007	D_4=296.754	E_4=1.97E+03
B_5=-0.14729	C_5=-82.7347	D_5=-118.9451	E_5=-705.0072

By calculating the polynomials of α, A, n, and Q value under different strain, the Z parameter under various conditions can be calculated. Substituting the Z parameter into equation (8), the stress value σ at different temperature, strain rate and strain are obtained, with the comparison of the experimental stress data, in Figure 4.

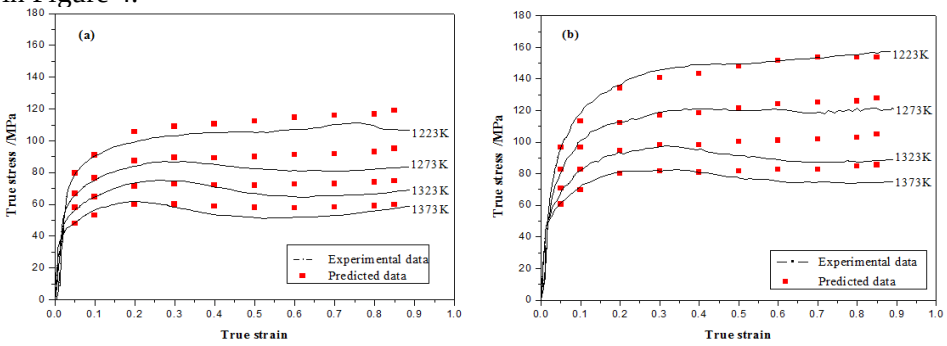

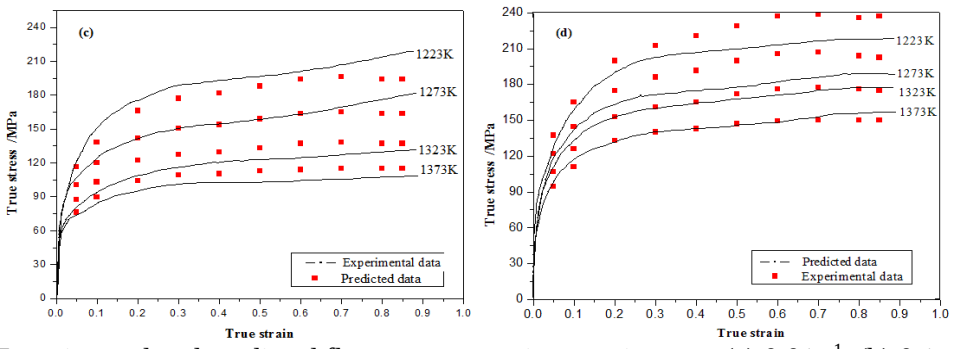

Figure 4 Experimental and predicted flow stress at various strain rates: (a) $0.01s^{-1}$, (b) $0.1s^{-1}$, (c) $1s^{-1}$, (d) $10s^{-1}$.

As can be seen from Figure 4, when the strain rate is (0.01 ~ 1) s^{-1}, the experimental value is in line with the predicted value. When the strain rate is $10s^{-1}$ and strain is greater than 0.4, the error becomes larger, that's because that the insulation shear zone is formed inside the material under the higher strain rate [17].

Assuming that the material constants (i.e. α, n, lnA and Q) are polynomial function of strains [18], [19] and [20], the constitutive equation of 0Cr11Ni2MoVNb stainless steel considering the effect of strain on flow stress was finally evaluated, a fifth order polynomial was adopted to describe to the influence of strain.

3.3 Verification of the developed constitutive equation

The accuracy of the constitutive equation is verified by statistical correlation coefficient (R) and the average absolute relative error (AARE). The calculation formula is as follows [21, 22]:

$$R = \frac{\sum_{i=1}^{n}(E_i - \bar{E})(P_i - \bar{P})}{\sqrt{\sum_{i=1}^{n}(E_i - \bar{E})^2 \sum_{i=1}^{n}(P_i - \bar{P})^2}} \tag{11}$$

$$AARE(\%) = \frac{1}{N}\sum_{i=1}^{N}\left|\frac{E_i - P_i}{E_i}\right| \times 100 \tag{12}$$

Where P is the predicted flow stress, E is the experimental flow stress, $\bar{P}$ and $\bar{E}$ is the mean values of P and E respectively. R is a commonly statistical parameter, which reflects a linear relationship between the experimental and predicted data. N is the total number of data.

The accuracy of the constitutive equation is verified by statistical correlation coefficient (R) and the average absolute relative error (AARE). The *AARE* value calculated through a comparison of predicted flow stress and experimental one is used to determine the predictability of the constitutive equation considering strain compensation. Comparison of experimental and predicted flow stress from constitutive equation is in Figure 5.

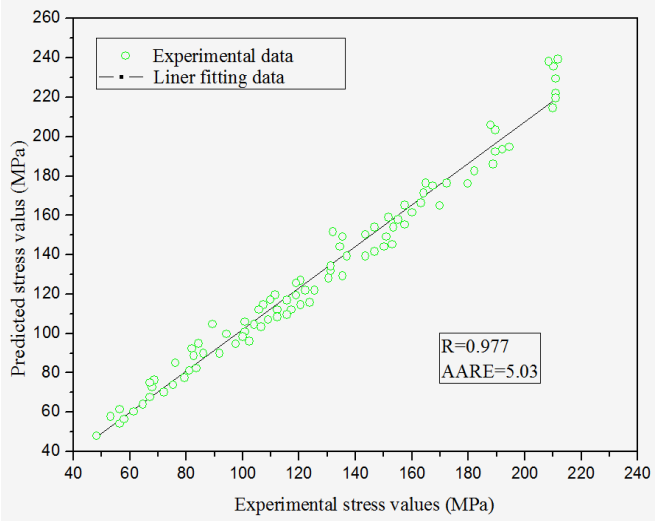

Figure 5 Correlation between experimental flow stress and data predicted from constitutive equation

As is in Figure 5, experimental flow stress and predicted data from constitutive equation turn on a strong correlation, the higher the stress is under lower deformation temperature and higher strain rate, the stronger the variation is. Though variation with relative error at part of curves exists, the values of *R* and *AARE* were merely 0.977% and 5.031% respectively. Thus the constitutive equation considering strain compensation reflects a good prediction capability of true flow stress.

4. Conclusion

The isothermal compression experiment is carried out on the Gleeble-1500 machine for the specimen of the 0Cr11Ni2MoVNb martensitic stainless steel, through the data analysis and calculation, hot forming properties and rheological behavior of the steel was studied and the constitutive equation is obtained. Results are as:

(1) 0Cr11Ni$_2$MoVNb steel is sensitive to temperature and strain rate. Within the test temperature range, the lower the temperature is and the higher the strain rate is, the greater the flow stress is. Besides, at high temperature, the hardening effect is not obvious and the dynamic response appears. Moreover, the softening of yield appears under high temperature and low strain rate.

(2) In the constitutive analysis, the effect of strain on the material constants (including α, n, lnA, Q, etc.) is considered, and it has good correlation and universality for the constant expression of constitutive equation by the five times polynomial associated with strain.

(3) Considering the compensation of strain, constitutive equation can accurately predict the stress value under different conditions of temperature and strain rate. Although constitutive equation has certain deviation in a certain degree, it is still within the acceptable error range, thus can better reflect the material change rules and characteristics of the stress-strain curve.

(4) The constitutive equation of 0Cr11Ni2MoVNb steel is established, which is as follows:

$$\dot{\varepsilon} = 1.8926\times10^{16}\left[\sinh\left(0.009206\sigma\right)\right]^{6.7015}\exp\left(\frac{-432078}{RT}\right)$$

The deformation activation energy of the 0Cr11Ni2MoVNb steel was obtained, Q=432.078kJ/mol. The material processing parameters and steady flow stress of the 0Cr11Ni2MoVNb steel are calculated.

Acknowledgements

This work is supported by Natural Science Foundation of China (No.51275414). Thanks to the ANDA Aviation Forging Co., Ltd. for the financial support. Thanks to Qiufeng WANG for her help. Also great thank to the Aviation Industry Corporation of China (AVIC) for the experimental instruction.

References

[1] Lo K H, Shek C H, Lai J K L. Recent developments in stainless steels[J]. Materials Science and Engineering: R: Reports, 2009, 65(4): 39-104.
[2] Müller-B. C, Zimmermann M, Christ H J. Adjusting the very high cycle fatigue properties of a metastable austenitic stainless steel by means of the martensite content[J]. Procedia Engineering, 2010, 2(1): 1663-1672.
[3] Fu J, B. Fabrice , K.B. Siham, Assessment of the elastic properties of amorphous Calcium Silicates Hydrates (I) and (II) structures by Molecular Dynamics Simulation[J]. Molecular Simulation.2017, 44(05):1-15.
[4] Fu J, B. Fabrice, K.B. Siham. First-principles calculations of typical anisotropic cubic and hexagonal structures and homogenized moduli estimation based on the Y-parameter[J]. Journal of Physics and Chemistry of Solids, 2017, 101: 74-89.
[5] Fu J, B. Fabrice, K.B. Siham, Multiscale Modeling and Mechanical Properties of Zigzag CNT and Triple-Layer Graphene Sheet Based on Atomic Finite Element Method[J]. J. Nano Research. 2015, 33:92-105
[6] Fu J, Yongtang Li, Huiping Qi. Microstructure simulation and experimental research of as-cast 42CrMo steel during quenching process, Advanced Materials Research, 2011, (317-319):19-23.
[7] Fu J, Li F, Li Y, et al. Microstructure simulation and mechanical properties of aisi1050 disk during quenching process[J]. The 2016 International Conference on Innovative Material Science and Technology,2016.
[8] Ji G, Li F, Li Q, et al. Research on the dynamic recrystallization kinetics of Aermet100 steel[J]. Materials Science and Engineering: A, 2010, 527(9): 2350-2355.
[9] Ji G, Li F, Li Q, et al. Prediction of the hot deformation behavior for Aermet100 steel using an artificial neural network[J]. Computational Materials Science, 2010, 48(3): 626-632.
[10] Ji G, Li F, Li Q, et al. A comparative study on Arrhenius-type constitutive model and artificial neural network model to predict high-temperature deformation behaviour in Aermet100 steel[J]. Materials Science and Engineering: A, 2011, 528(13): 4774-4782.
[11] Y.C.Lin，Ming -Song Chen,Jue Zhong, Effect of temperature andstrain rate on the compressive deformation behavior of 42CrMo steel[J]. Journal of Materials Processing Technology, 2008, 205(1 -3): 308-315.
[12] Sumantra Mandal, V. Rakesh, et al..Constitutive equations to predict high temperature flow stress in a Ti -modified austenitic stainless steel [J]. Materials Science and Engineering:A, 2009, 500(1-2):114-121.
[13] Y.C.Lin, Ming-Song Chen, Jue Zhong. Constitutive modeling for elevated temperature flow behavior of 42CrMo steel[J]. Computational Materials Science, 2008, 42(3): 470-477.
[14] Cheng Y Q, Zhang H, Chen Z H, et al. Flow stress equation of AZ31 magnesium alloy sheet during warm tensile deformation[J]. Journal of materials processing technology, 2008, 208(1): 29-34.
[15] Gao H, Barber G C, Chen Q A, et al. High temperature deformation of a Fe-based low nickel alloy[J]. Journal of Materials Processing Technology, 2003, 142(1): 52-57.
[16] Sellars C M, et al. On the mechanism of hot deformation[J]. Acta Metallurgica, 1966, 14(9): 1136-1138.
[17] Y.C.Lin，Ming -Song Chena，Jue Zhong. Prediction of 42CrMo steel flow stress at high temperature and strain rate [J]. Mechanics Research Communications, 2008, 35(3): 142-150.
[18] Samantaray D, Mandal S, Bhaduri A K. Constitutive analysis to predict high-temperature flow stress in modified 9Cr–1Mo (P91) steel[J]. Materials & Design, 2010, 31(2): 981-984.
[19] Lin Y C, Chen M S, Zhong J. Constitutive modeling for elevated temperature flow behavior of 42CrMo steel[J]. Computational Materials Science, 2008, 42(3): 470-477.

[20] Mandal S, Rakesh V, Sivaprasad P V, et al. Constitutive equations to predict high temperature flow stress in a Ti-modified austenitic stainless steel[J]. Materials Science and Engineering: A, 2009, 500(1): 114-121.
[21] Li H Y, Wang X F, Wei D D, et al. A comparative study on modified Zerilli–Armstrong, Arrhenius-type and artificial neural network models to predict high-temperature deformation behavior in T24 steel[J]. Materials Science and Engineering: A, 2012, 536: 216-222.
[22] Li J, Li F, Cai J, et al. Flow behavior modeling of the 7050 aluminum alloy at elevated temperatures considering the compensation of strain[J]. Materials & Design, 2012, 42: 369-377.